

# Comparison of Oxidants Used in Advanced Oxidation for Potable Reuse: Non-Target Analysis and Bioassays

Mingrui Song, Elizabeth McKenna, Imma Ferrer, E. Michael Thurman, Liz Taylor-Edmonds, Ronald Hofmann, Kenneth P. Ishida, Shannon L. Roback, Megan H. Plumlee, and David Hanigan\*



Cite This: *ACS EST Water* 2023, 3, 690–700



Read Online

ACCESS |

Metrics & More

Article Recommendations

Supporting Information

**ABSTRACT:** Free chlorine (HOCl) and monochloramine (NH<sub>2</sub>Cl) are less-used oxidants than hydrogen peroxide (H<sub>2</sub>O<sub>2</sub>) in ultraviolet advanced oxidation processes (UV-AOPs) but have garnered interest from the water reuse industry and scientific community because they can be more cost-effective than H<sub>2</sub>O<sub>2</sub> and provide a protective disinfectant residual. The destruction of organic compounds, creation of UV-AOP byproducts, and change in toxicity during UV-AOP with H<sub>2</sub>O<sub>2</sub>, HOCl, NH<sub>2</sub>Cl, or ambient residual chloramine were evaluated in recycled wastewater by suspect and non-target screening as well as bioanalytical tests (bioassays). Ten compounds were identified in reverse osmosis (RO) permeate via suspect screening with removal near 100% by UV/H<sub>2</sub>O<sub>2</sub> and UV/HOCl, greater than decomposition by UV/NH<sub>2</sub>Cl and UV/ambient (~60%), based on suspect screening mass spectrometry peak area. Non-target analysis based on organic features in mixed-mode cation exchange cartridge extracts indicated that UV/H<sub>2</sub>O<sub>2</sub> destroyed a similar or slightly greater fraction of organic compounds, formed fewer transformation products, and reduced the summed peak area of non-target features to the greatest extent. Fewer chlorinated byproducts were produced from the RO permeate treated by UV/H<sub>2</sub>O<sub>2</sub> than exposure to the chlorine-containing oxidants. Addition of NH<sub>2</sub>Cl to RO permeate resulted in a slight increase in the bioassay oxidative stress response but dropped below the response limit for all samples after UV-AOP for all oxidants.

**KEYWORDS:** monochloramine, free chlorine, hydrogen peroxide, disinfection byproduct, indirect potable reuse, bioassays, non-target

## 1. INTRODUCTION

Planned potable reuse has been employed for decades to relieve water scarcity.<sup>1,2</sup> Various treatment trains based on the combinations of ozone, soil aquifer treatment, biological activated carbon, membranes, and ultraviolet advanced oxidation process (UV-AOP) are designed with the intent to degrade or remove contaminants present in conventional wastewater effluents.<sup>3</sup> Full-advanced treatment (FAT) defined by California State Water Resources Control Board<sup>3,4</sup> is a common treatment train and consists of ultrafiltration (UF) or microfiltration (MF) followed by reverse osmosis (RO) as a broad-screen physical removal process. A UV-AOP is then employed to provide disinfection and destruction of remaining organic compounds that are incompletely rejected by RO.

Hydrogen peroxide (H<sub>2</sub>O<sub>2</sub>) is a commonly added oxidant for UV-AOP because it produces highly reactive hydroxyl radicals when exposed to UV light.<sup>3</sup> Free chlorine (HOCl) is an alternative oxidant that may be coupled with UV that has garnered interest from the water reuse industry and scientific community due to certain practical advantages over H<sub>2</sub>O<sub>2</sub>: the low cost of sodium hypochlorite and the ability to avoid quenching the H<sub>2</sub>O<sub>2</sub> residual in the finished water when removal is required prior to distribution. Another advantage is the on-site availability and familiarity of hypochlorite since it is often used to form chloramines to control membrane

biofouling<sup>5</sup> and disinfect the finished water while providing a protective residual for distribution.<sup>6</sup>

Chloramines for control of biofouling are readily formed when sodium hypochlorite is added to the secondary- or tertiary-treated wastewater effluent containing residual ammonia. Chloramines are poorly rejected by RO,<sup>7</sup> and therefore, UV/H<sub>2</sub>O<sub>2</sub> is de facto UV/H<sub>2</sub>O<sub>2</sub>/chloramine AOP. Photolysis of monochloramine (NH<sub>2</sub>Cl) and dichloramine (NHCl<sub>2</sub>) produces reactive chlorine, amine, and peroxide radicals, which degrade organic compounds.<sup>8–10</sup> However, during UV-AOP, residual chloramines from upstream treatment also compete with added H<sub>2</sub>O<sub>2</sub> or free chlorine for photons and scavenge hydroxyl radicals, decreasing AOP efficiency.<sup>5,6</sup> Nevertheless, because NH<sub>2</sub>Cl is already present in the source water, use of supplemental NH<sub>2</sub>Cl as a primary UV-AOP oxidant may reduce costs and has therefore received some attention from UV-AOP system operators and scientists.<sup>9</sup>

Received: September 28, 2022

Revised: January 19, 2023

Accepted: January 20, 2023

Published: February 6, 2023



Certain pharmaceuticals have been shown to be poorly degraded by UV-AOP with  $\text{H}_2\text{O}_2$ , including metformin, cyclophosphamide, and ifosfamide,<sup>11</sup> and incomplete compound elimination during UV-AOP may result in transformation products, which, in some instances, are more toxic than the parent compounds.<sup>12–14</sup> Precursors of *N*-nitrosodimethylamine (NDMA), a carcinogenic disinfection byproduct, are only partially removed by UV-AOP, and their rejection by RO has been shown to decrease with increasing RO membrane age, increasing the potential for NDMA to form in potable reuse water after FAT.<sup>15,16</sup> At higher concentrations, these incompletely removed compounds may pose a threat to human health,<sup>11,17</sup> and even at low concentrations, they diminish social acceptance of the finished water.

Most studies that have investigated the degradation of organic compounds during potable reuse have focused on measuring or detecting preselected “target” organic compounds<sup>9,18,19</sup> such as pharmaceuticals and individual DBP precursors. However, unknown and previously unmonitored organic compounds may also be present with the potential to cause unanticipated adverse effects.<sup>20,21</sup> The availability of analytical methods may lead to overemphasis of the importance of a particular organic compound, including the benchmarking and ranking of treatment technologies against one another based on their performance for removal of somewhat arbitrary compounds—the proverbial “tail that wags the dog”. Thus, improved methods are needed to meaningfully assess water quality and subsequent determination of their potential impact on public health through further studies.

Liquid chromatography (LC) or gas chromatography (GC) coupled to high-resolution mass spectrometry (HRMS) provides simultaneous detection of thousands of compounds, including known and unknown chemicals. Suspect screening is conducted by searching of a chemical database (prior information) for molecular weight, fragmentation pattern, and potential retention time matches to identify contaminants. Non-target analysis (NTA) is a separate method of identifying unknown chemicals by their mass to charge ratio alone without prior information.<sup>22</sup> Some studies have utilized NTA to investigate the occurrence of organic contaminants at potable reuse facilities.<sup>16,23–26</sup> However, there are few NTA studies that have sought to investigate the fraction of organic compounds that persist through potable reuse, and thus, the composition of these recalcitrant organic compounds is relatively unknown. In addition to chemical analysis, *in vitro* bioassays have been proposed to assess water quality.<sup>27</sup> Bioassays produce dose–response curves that can be used to benchmark bulk water quality as a complement to chemical analysis, which only detects target compounds or, for NTA, which only detects those organic molecules that are measurable by mass spectrometry.<sup>28</sup> Studies using bioassays have emphasized the agonistic and antagonistic effects of mixtures of compounds, including contributions from unidentified organic compounds,<sup>29–32</sup> and these effects are not directly captured by HRMS approaches. Further, there is currently no consensus as to which bioassay(s) is an appropriate surrogate for risk to human health.

To determine the relative performance of HOCl,  $\text{H}_2\text{O}_2$ , and  $\text{NH}_2\text{Cl}$  oxidants during UV-AOP, we utilized suspect screening and non-target analysis as well as *in vitro* bioassays. These tools were applied to the subset of organic matter recovered from product water of a pilot UV-AOP system operated at the Orange County Water District (OCWD) Groundwater

Replenishment System (GWRS) Advanced Water Purification Facility (AWPF) that treated RO permeate from the full-scale plant. The reuse facility is broadly representative of many FAT plants that treat secondary and tertiary wastewater by MF/UF and RO. Our objectives were to (1) determine which suspect compounds are present in the treated wastewater, i.e., RO permeate, and the extent to which they are degraded with various radical forming oxidants during UV-AOP, (2) compare the removal of non-target features based on the type of oxidant and the generation of new UV-AOP byproducts, and (3) assess the changes to bioassay-measured toxicity before and after UV-AOP with various oxidants.

## 2. MATERIALS AND METHODS

**2.1. Chemicals and Reagents.** HPLC-grade solvents (methanol, acetonitrile, and methylene chloride) and ascorbic acid were purchased from Fisher Scientific (Pittsburgh, PA). Hydrogen peroxide (30% w/w), sodium hypochlorite (10–15%), and ammonium hydroxide were purchased from Sigma-Aldrich (St. Louis, MO). Reagent water was either  $\geq 18.2 \text{ M}\Omega \text{ cm}$  (Milli-Q) or HPLC-grade (Fisher Scientific). Two types of solid-phase extraction (SPE) cartridges commonly utilized for recovering organics were used to produce isolates: mixed-mode cation exchange (MCX) 6 mL/500 mg for non-target analysis and hydrophilic–lipophilic balance (HLB) and 6 mL/200 mg (Oasis, Waters Corporation, MA) for bioassay analysis.<sup>33,34</sup> The SPE isolates are representative of subsets of the organic matter pool. In these experiments, the MCX sorbent was selected for mass spectrometry experiments because we previously demonstrated that organic bases, which are a large subset of compounds amenable to positive electrospray ionization (i.e., cations, polar compounds, moderately polar compounds, etc.), are captured and recovered well by MCX resin via cation exchange but not by the HLB resin.<sup>35,36</sup> Further, MCX resins are “mixed-mode” and capture bases in addition to nonpolar compounds, and we have previously demonstrated good recovery of compounds which are of broad importance to potable reuse utilities (NDMA precursors).<sup>35</sup> The HLB sorbent was used to capture a broad range of organic compounds for bioassay experiments.<sup>37</sup> An important limitation of the methods is that all extraction methods of organic matter result in potential biases of the conclusion related to the inadvertent fractionation of organic matter (sorbent affinity, ionization efficiency, etc.) Sulfuric acid (Fisher Scientific) was used to adjust the sample pH.

**2.2. Sample Collection and Extraction.** Samples were collected on two occasions (August 2018 and September 2019) from a pilot UV-AOP reactor fed with reverse osmosis permeate (ROP) from the full-scale GWRS AWPF in Fountain Valley, California. The AWPF treats secondary wastewater effluent from the Orange County Sanitation District (OC San) by MF or UF (installed in different, parallel cells), RO, and UV-AOP to produce high-purity water for groundwater recharge via spreading (percolation) ponds, mid-basin injection wells, and injection into a coastal seawater intrusion barrier. Ultimately, this groundwater augmentation is pumped by local water retailers via production wells for drinking water use, i.e., indirect potable reuse.

Sampling locations for ROP, UV feed (UVF), and UV product (UVP) are shown in Figure S1. The pilot UV system was composed of a 9.7 L stainless steel reactor with a 257 W low-pressure high-output mercury amalgam lamp (Trojan Technologies, London, Ontario, Canada). The flow rate

through the reactor was 22.7 L/min (6 gpm) with a residence time in contact with the oxidant (inline mixer injection point to UVF) of  $\sim 3$  s and UV exposure (between UVF and UVP) of 26 s. The operation of the pilot UV reactor and preparation of oxidant solutions are described in detail in Zhang et al.<sup>7</sup> Working solutions of HOCl, H<sub>2</sub>O<sub>2</sub>, and NH<sub>2</sub>Cl were delivered by peristaltic pump into the ROP through an inline static mixer (Koflo, Cary, IL) to achieve the target dose.

Grab samples (1 L) of the ROP, UVF, and UVP were collected in 2018 and 2019 during separate UV-AOP pilot trials. In 2018 UV-AOP pilot trials, either no additional oxidant was added to the ROP or one of three individual oxidants (HOCl, H<sub>2</sub>O<sub>2</sub>, or NH<sub>2</sub>Cl) were added to the ROP prior to exposure to UV light, producing four sets of UV-AOP samples. We refer to these combinations of oxidants as UV/HOCl, UV/H<sub>2</sub>O<sub>2</sub>, UV/NH<sub>2</sub>Cl, and UV/ambient, where "UV/ambient" refers to UV-AOP with only the residual chloramines in the ROP as the oxidant and "UV/NH<sub>2</sub>Cl" refers to supplemental addition of NH<sub>2</sub>Cl to the ROP. Residual chloramines for biofouling control are always present in the ROP and therefore also present when supplemental oxidant is added to form the UVF to the reactor. In 2019 UV-AOP pilot trials, only HOCl and H<sub>2</sub>O<sub>2</sub> were dosed into the ROP to validate the more promising oxidants from the 2018 trials. A summary of the sample information and general water quality data is provided in Table S1. The pH of ROP was  $5.8 \pm 0.2$ , which is near the optimal pH for UV/HOCl.<sup>38</sup> Although there are some studies investigating the effect of pH on organic degradation for UV/NH<sub>2</sub>Cl, the suggested optimal pH is variable.<sup>39,40</sup> Hence, we made the reasonable and economical (for full-scale design) decision to leave the pH unchanged.

Residual total chlorine (Hach Co., Method 10070) in the grab samples was measured immediately and quenched with a 1.2 molar excess of ascorbic acid. The hydrogen peroxide and residual chloramines were quenched with 100 mg of ascorbic acid added to each bottle prior to sample collection. In addition, free chlorine (Hach Co., Method 10241), monochloramine (Hach Co., Method 10171), ammonia (Hach Co., Method 10200), UV transmittance (UVT) at 254 nm, and pH were measured. Samples and field blanks (consisting of a new bottle of Burdick & Jackson LC-MS grade water opened and poured into 1 L sample bottles on site) were immediately shipped on ice to the University of Nevada, Reno (UNR). The field blanks or blanks of Milli-Q water ( $\geq 18 \text{ M}\Omega \text{ cm}$ ) were extracted to assess potential contamination from reagent water. Samples were extracted at UNR with MCX cartridges by previous established methods<sup>35</sup> and sent to University of Colorado, Boulder (CU) overnight on ice. As is typical in suspect screening and non-target analysis, a surrogate standard was not added to account for recovery because no individual standard (or even multiple standards) will appropriately account for the recovery of the thousands of compounds that were to be measured. Further, it is not possible to know what will be discovered during the analysis, and thus, it is not possible to anticipate which surrogate may be appropriate to add. Further details are provided in the Supporting Information Text S1. Water parameters including DOC and anions are not provided due to the low concentrations after RO treatment and the difficulty measuring such low concentrations.

Samples collected for bioassays were quenched with a 2.5 molar excess of ascorbic acid and shipped to the University of Toronto. The usage of quenching agents was in accordance

with standard procedures for each individual lab. SPE was conducted on duplicate aliquots with 200 mg HLB cartridges. Two liters of acidified sample (pH 2) were loaded on the cartridge, eluted with 10 mL of acetone, and evaporated under a gentle ultrahigh-purity nitrogen stream. Samples were reconstituted in 100  $\mu\text{L}$  of methanol for subsequent cellular testing. Detailed procedures can be found in Zheng et al.<sup>41</sup> For comparison of bioanalytical activity to a typical finished drinking water, Otonabee River water was collected after coagulation, flocculation, and filtration from a conventional drinking water treatment plant and subjected to bench chlorination (5 mg/L as Cl<sub>2</sub> for 24 h at room temperature). The chlorine dose mimicked the upper limit disinfection dose of the full-scale plant. Chlorine was quenched after 24 h with ascorbic acid, and the samples were extracted.

**2.3. Instrumental Analysis.** Extracts from MCX cartridges were analyzed by an LC system consisting of a vacuum degasser, thermostatted autosampler, column compartment, and binary pump (Agilent Series 1290, Agilent Technologies, Santa Clara, CA, USA) coupled to an Agilent 6545 ultrahigh-definition quadrupole time-of-flight mass spectrometer (qTOF/MS, Agilent Technologies, Santa Clara, CA, USA) with electrospray Jet Stream Technology. Isolates were diluted 10-fold into Milli-Q water prior to injection to facilitate chromatographic separation by a reversed-phase C8 analytical column (150 mm  $\times$  4.6 mm) with a 3.5  $\mu\text{m}$  particle size (Zorbax Eclipse XDB-C8). For quality assurance and control, stability of mass accuracy was checked daily, and if values were above 2 ppm error, the instrument was recalibrated. Further details regarding operation parameters and mass stability check are provided in the Supporting Information Text S1.

**2.4. Data Analysis.** MassHunter software was initially utilized to conduct suspect screening with LC-qTOF/MS data. Suspect screening was conducted by matching the retention time, accurate mass, fragmentation pattern, and the isotope abundance ratios to two in-house databases at CU; one containing over 100 pharmaceuticals and pesticides and another containing approximately 60 known *N*-nitrosamine precursors. In prior experiments with this instrument, molecular features with high scores (>80, full score 100) were nearly always a correct hit. Matches with a score of <80 were disregarded.

Raw data files were converted into a centroided mzML format by MSConvert software (ProteoWizard, Palo Alto, CA). Processing non-target features included the construction of extracted ion chromatograms (EIC) and peak detection performed by the automated data analysis pipeline within MZmine 2.<sup>42</sup> Other non-target feature processing such as grouping and retention time algorithms were conducted using methods described by Verkh et al.<sup>43</sup> Preprocessing parameters of peak detection, EIC building, and peak picking for all data files is summarized in Table S2. Only features (i.e., unique peaks) present in samples with a peak area of at least three times greater than those present in the field and Milli-Q blanks are reported. Summed peak area of the non-target features was obtained by summing the peak area of all qualified features in the sample.

Molecular formulae were assigned by MZmine 2.<sup>44</sup> The ionization type was  $[\text{M} + \text{H}]^+$  with a charge of +1, and the mass tolerance was 0.005  $m/z$ . The possible ranges of each element in the formulae were: C<sub>1–80</sub>, H<sub>1–100</sub>, O<sub>1–30</sub>, N<sub>0–3</sub>, S<sub>0–2</sub>, and Cl<sub>0–4</sub>. Element count heuristics and ring double-bond equivalent restrictions of 0–40 were applied during formula

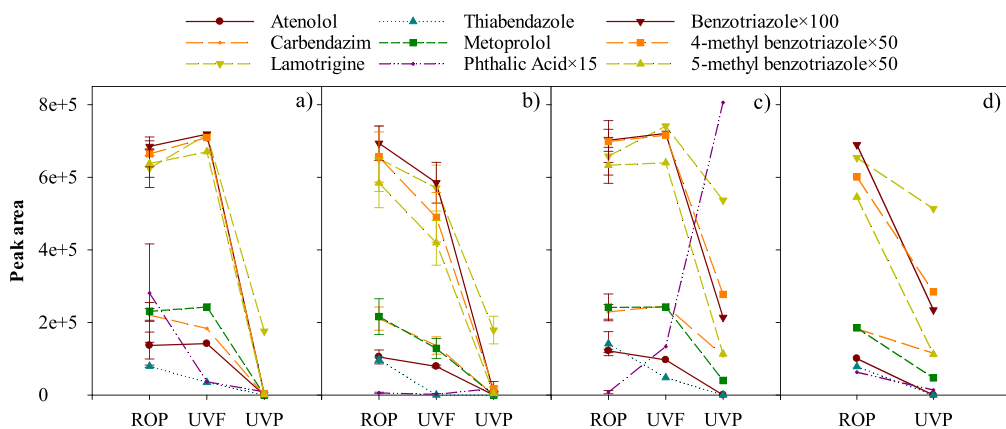


**Figure 1.** Peak area of suspect compounds in MCX extracts of samples from 2018 ROP, UVF, and UVP treated by a) UV/HOCl, b) UV/H<sub>2</sub>O<sub>2</sub>, c) UV/NH<sub>2</sub>Cl, and d) UV/ambient. For panel (d), UVF was not sampled because no supplemental oxidant was added to the ROP. Compound  $\times$  factor indicates the offset of the data for clarity. The error bars indicate the range of duplicates. Suspect compound peak area from the 2019 UV-AOP pilot sampling event is available in **Figure S2**.

prediction. All results were exported to CSV format by MZmine 2. Blank subtraction was performed in R Studio.<sup>45</sup>

**2.5. Bioassays.** Bioassays (Table S3) were selected to provide a broad-spectrum screening of various adaptive stress response pathways that are relevant to drinking water treatment including general cellular stress (p53), oxidative stress (ARE-Nrf2), and genotoxicity (SOS Chromotest). Cytotoxicity was measured by conversion of dye-based cytotoxicity assay (MTT); the detailed procedure is presented in Sun et al.<sup>46</sup> The human cell-based ARE-Nrf2 assay targets the activation of the oxidative stress response pathway. Detailed methods are described by Sun et al.<sup>46</sup> Activation of the DNA repair pathway mediated by the SOS-response pathway was performed to measure DNA damage using the SOS Chromotest (EBPI Inc) assay. Detailed methods are described in Zheng et al.<sup>41</sup> p53 was also assayed as this assay is responsive to general cellular stress and involved in apoptosis signaling.<sup>47</sup> Methods are described in Sun et al.<sup>46</sup>

For the luciferase reporter assays fused to ARE-Nrf2 and p53 response element operons, activation of the pathway is expressed as an induction ratio (IR) of treated cells compared to control, where an IR of  $\geq 1.5$  was considered a positive response. For positive samples, effect concentrations (EC) for IRs of 1.5 were derived from the linear slopes of the dose-response curves, where the concentrations correspond to the relative enrichment factor.<sup>48</sup> Thus, EC<sub>IR1.5</sub> corresponds to how many times the sample must be concentrated or diluted to elicit an IR of 1.5. Further details are presented in Escher et al.<sup>48</sup> The results are expressed as 1/EC<sub>IR1.5</sub> and referred to as toxicity units (TU); a higher TU represents a greater toxic effect. The bioassay limit of detection (LOD) is 0.018 TU.

Similarly, the SOS Chromotest response was determined as the induction ratio of the  $\beta$ -galactosidase ( $\beta$ -gal) reporter gene fused to the bacterial SOS operon. In addition, general protein synthesis was measured using the photometric quantification of alkaline phosphatase (AP). The induction of  $\beta$ -gal is indicative of the DNA damage and was expressed as the ratio of  $\beta$ -gal activity to AP activity, which is referred to as the induction factor (IF). An IF of  $\geq 1.5$  was considered positive in the genotoxicity assay. For cytotoxicity, samples with cell viabilities greater than 80% were considered for toxicity bioassay assessment.

### 3. RESULTS AND DISCUSSION

**3.1. Suspect Compounds.** Across 28 water samples spanning the full treatment train (ROP, UVF, and UVP) over two sampling events and including 4 field blanks, a total of 10 compounds were identified via suspect screening from a mass spectrometry library of over 160 compounds (Table S4). The compounds of the in-house library are provided in a previous work by our team.<sup>16,49–51</sup> Six of the ten compounds were detected in samples from both 2018 and 2019: benzotriazole and two methylated benzotriazoles (anti-corrosion agents), atenolol and metoprolol (blood pressure medications), and lamotrigine (anti-seizure medication). Three compounds were identified only in samples from 2018: phthalic acid (plasticizer) and thiabendazole and carbendazim (fungicide). Sucralose (artificial sweetener) was only identified in samples from 2019.

The peak areas of suspect compounds that were present in the ROP, UVF, and UVP samples under varying oxidant conditions are shown in Figure 1 for the 2018 UV-AOP pilot sampling event. Although the peak area is subject to ionization matrix effects (and no surrogates were added to the samples prior to extraction to correct for this) and, thus, comparisons between samples are only semi-quantitative, we have previously shown that the matrix effects are minimal in similar extracts as salts are removed during the MCX extraction and most organic matter is removed by the RO membranes.<sup>16</sup> As is typical in suspect screening and non-target analysis, a surrogate standard was not added to account for recovery because no individual standard (or even multiple standards) will appropriately account for recovery of the thousands of compounds that were to be measured. Further, it is not possible to know what will be discovered during the analysis, and thus, it is not possible to anticipate which surrogate may be appropriate to add. Trends from 2018 were similar to 2019 (Figure S2), except that fewer suspect compounds were detected in 2019. Rapid oxidation by H<sub>2</sub>O<sub>2</sub> prior to exposure to UV light was somewhat greater than other oxidants. After  $\sim 3$  s of exposure to 2.9 mg/L H<sub>2</sub>O<sub>2</sub> (2018) and 2.8 mg/L (2019), the summed peak area of the suspect compounds in ROP dropped 21% and 8%, respectively, while less than a 2% reduction in the summed peak area (Table S5) was observed by exposure to 2.0 mg/L HOCl (2018), 2.3 mg/L (2019) HOCl, and 2.2 mg/L NH<sub>2</sub>Cl (2018). These oxidant doses

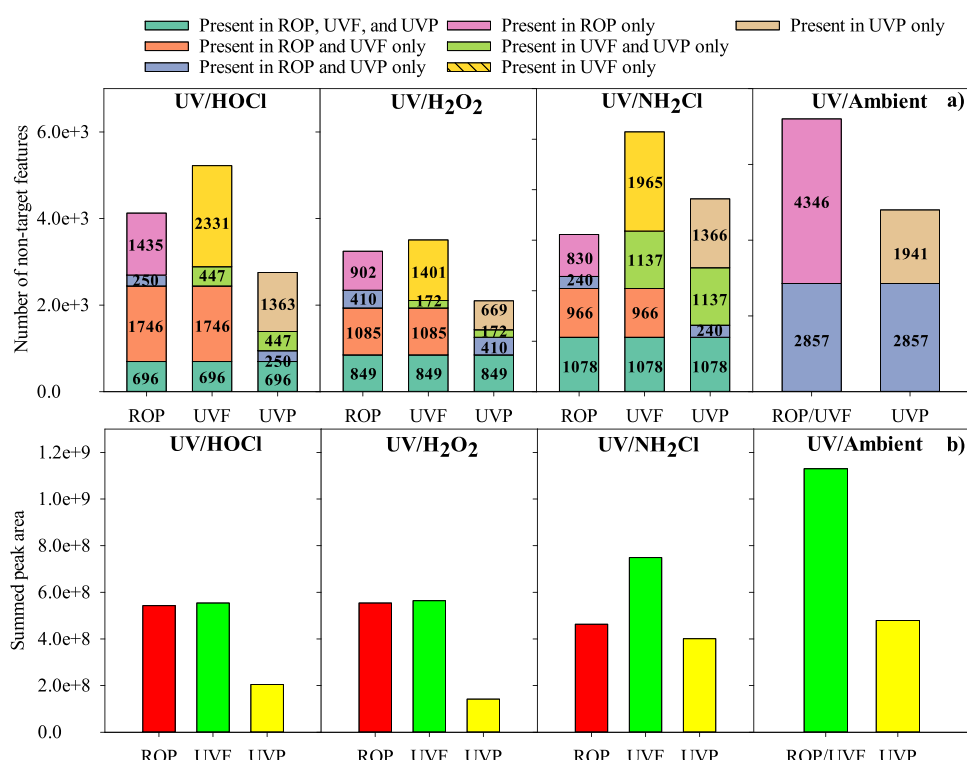


**Figure 2.** Plots of a) number and b) summed peak area of all non-target features across the pilot-scale UV-AOP in 2018.

represent likely concentrations used in water reuse plants with UV-AOP.

For UV/HOCl and UV/NH<sub>2</sub>Cl, the peak areas of atenolol, lamotrigine, metoprolol, benzotriazole, and two methylated benzotriazoles detected in ROP were unchanged by exposure to HOCl and NH<sub>2</sub>Cl, indicating that these compounds were recalcitrant to rapid oxidation by low concentrations of these oxidants (Figure 1a,c and Figure S2a). This trend was consistent with the results of similar studies, where atenolol, metoprolol, and benzotriazole were poorly degraded by chlorination.<sup>52–54</sup>

For the 2018 sampling event, the summed peak area of all suspect compounds recovered from ROP was reduced 99%, 98%, 66%, and 61% by UV/HOCl, UV/H<sub>2</sub>O<sub>2</sub>, UV/ambient, and UV/NH<sub>2</sub>Cl, respectively (Table S5). The percent reduction of the summed peak areas for both UV/HOCl and UV/H<sub>2</sub>O<sub>2</sub> were similar for the 2019 sampling event (Figure S2). Other studies have also reported that degradation of the relatively recalcitrant organic compounds 1,4-dioxane and iopamidol by UV/HOCl and UV/H<sub>2</sub>O<sub>2</sub> is greater than UV/NH<sub>2</sub>Cl.<sup>7,55</sup> Notably, the peak area of phthalic acid increased ~5× across UV/H<sub>2</sub>O<sub>2</sub> (Figure 1b) and UV/NH<sub>2</sub>Cl (Figure 1c). Because the peak area of phthalic acid was small in UVF samples, which are taken after oxidant addition, the phthalic acid was not from the oxidant solutions. It was likely produced via the oxidation or photolysis of phthalates,<sup>56</sup> and this phenomenon highlights that some compounds are not removed completely but are transformed to new oxidation products. Overall, UV/HOCl and UV/H<sub>2</sub>O<sub>2</sub> were the most effective in terms of the removal of these suspect compounds over the two sampling events, and this agrees with the literature for difficult-to-degrade organic compounds.

### 3.2. Production and Persistence of Non-Target Features.

Non-target analysis was only conducted on samples processed from the 2018 event because the travel blank during

2019 was lost during shipment, making the necessary blank subtraction impossible. Bar plots of the number and summed peak areas of the non-target features from the ROP, UVF, and UVP samples are shown in Figure 2. UV/ambient conditions are only represented by ROP and UVP samples as no supplemental oxidant was added to the ROP prior to UV exposure. Samples were extracted with Oasis MCX cartridges, and the data is therefore representative of a large subset of the organic matter pool that is amenable to cation exchange and positive electrospray ionization (cations, polar compounds, moderately polar compounds, etc.).<sup>35,57</sup>

The total number of non-target features (i.e., unique peaks measured by mass spectrometry) in the feed water (ROP) ranged from 3114 to 7203. ROP samples before UV/H<sub>2</sub>O<sub>2</sub> and UV/NH<sub>2</sub>Cl were comparable (~3200) and less than UV/HOCl and UV/ambient, ~4100 and ~7200, respectively. Although the number of non-target features varied, the summed peak areas in the ROP before UV/HOCl, UV/H<sub>2</sub>O<sub>2</sub>, and UV/NH<sub>2</sub>Cl were comparable (4.6–5.5 × 10<sup>8</sup>), although the UV/ambient was 2–2.5 times greater in total peak area (1.13 × 10<sup>9</sup>). Variability in the number and peak area of features detected in the ROP samples is attributable to the natural variation in wastewater chemistry throughout the day in which the experiments were conducted. Thus, it is important to consider both the raw number (i.e., count) of features, their summed peak areas, and their percent removal/formation across the treatment train.

Across all oxidants, the number of non-target features in the UVF (ROP + oxidant, prior to UV exposure) was similar or greater than in the ROP, suggesting the formation of decomposition products by reactions with the oxidant. For example, for the UV/H<sub>2</sub>O<sub>2</sub> treatment, there were 3246 non-target features present in the ROP sample (Figure 2a). Comparing the features in the sample after contact with H<sub>2</sub>O<sub>2</sub>, we find a 48% increase (yellow plus bright green) in unique

features compared to the ROP sample (i.e., products of oxidation products). For HOCl and NH<sub>2</sub>Cl, the number of features in the UVF that were not present in the ROP sample increased by 67% and nearly 100%, respectively. In terms of the summed peak area of all features, after NH<sub>2</sub>Cl oxidation, the area increased by 62% (from  $4.6 \times 10^8$  to  $7.5 \times 10^8$ ) but was comparable ( $\leq 2\%$  difference) to HOCl and H<sub>2</sub>O<sub>2</sub> (Figure 2b). It is not clear why the number of non-target features increased but the summed peak area did not, but this may reflect that the number of compounds changed but the total mass of organic material did not change substantially and/or that the formation products from HOCl and H<sub>2</sub>O<sub>2</sub> are compounds which ionize poorly, reflecting the semi-quantitative nature of this approach.

Notably, a substantial portion of the features present in the ROP samples persisted after supplemental oxidant was applied (see Figure 2, dark green plus orange). A total of 2442 (59%) features were still detected in the UVF after HOCl addition, and 1934 (60%) and 2044 (66%) of features were still detectable after H<sub>2</sub>O<sub>2</sub> and NH<sub>2</sub>Cl exposure, respectively. Therefore, based on the feature (i.e., compound) count, brief exposure to HOCl and H<sub>2</sub>O<sub>2</sub> oxidation resulted in decomposition of a comparable fraction of non-target features and H<sub>2</sub>O<sub>2</sub> oxidation resulted in the least number/fraction of transformation products (albeit noting the fewer number of features in the ROF at that time for H<sub>2</sub>O<sub>2</sub>), followed by HOCl and NH<sub>2</sub>Cl. In terms of the summed peak area of non-target features, NH<sub>2</sub>Cl oxidation increased the peak area the most (62%), followed by HOCl and H<sub>2</sub>O<sub>2</sub> ( $\leq 2\%$ ).

After UV-AOP (from UVF to UVP), there was a reduction in the number of features regardless of the supplemented oxidant. The total number of non-target features in the UVF samples ranged from 3507–5220, which was reduced to 2100–3821 in the UVP (Figure 2a). There were 1143, 1021, and 2215 non-target features that persisted from UVF to UVP under UV-AOP conditions when HOCl, H<sub>2</sub>O<sub>2</sub>, and NH<sub>2</sub>Cl were added, respectively, and 2857 when no oxidant was added (ambient residual chloramines), accounting for 22%, 29%, 43%, and 40% of features in the corresponding UVF samples that were not completely removed by the UV-AOP. Stated differently, UV-AOP with HOCl, H<sub>2</sub>O<sub>2</sub>, NH<sub>2</sub>Cl, and ambient removed/decomposed 78%, 71%, 57%, and 60% of features from the UVF, respectively. The summed peak area from UVF to UVP of non-target features was reduced 63%, 75%, 46%, and 58% by UV/HOCl, UV/H<sub>2</sub>O<sub>2</sub>, UV/NH<sub>2</sub>Cl, and UV/ambient, respectively. This suggests that UV-AOP with H<sub>2</sub>O<sub>2</sub> or HOCl perform comparably (i.e., in this study, the feature count was reduced to a greater extent by HOCl, but more summed peak area was removed by H<sub>2</sub>O<sub>2</sub>) and better than residual chloramine or supplemental NH<sub>2</sub>Cl.

UV-AOP transformation products (new non-target features in the UVP, which were not present in UVF) were also evaluated. There were 1613, 1079, and 1606 newly formed non-target features after UV/HOCl, UV/H<sub>2</sub>O<sub>2</sub>, and UV/NH<sub>2</sub>Cl, equivalent to  $\sim 31\%$  new features regardless of which oxidant was added. UV/ambient formed 1941 new features or 27% new features. Note that UV/ambient formed the greatest number of UV-AOP transformation products, but the corresponding fractional increase in new features was the lowest of the four scenarios. This was likely caused by the greater number of non-target features in the corresponding UVF sample and demonstrates that percent changes are somewhat affected by the water quality of the UVF samples.

In terms of the overall reduction of the total count of non-target features across the pilot system from ROP to UVP, UV/HOCl, UV/H<sub>2</sub>O<sub>2</sub>, and UV/ambient performed similarly; the total number of non-target features was reduced by 33%, 35%, and 33% by UV/H<sub>2</sub>O<sub>2</sub>, UV/HOCl, and UV/ambient, respectively (Figure 2). The equivalent performance of UV/ambient compared to the added oxidants H<sub>2</sub>O<sub>2</sub> and HOCl is initially surprising. However, this is due to the net increase in feature count from ROP to UVF for H<sub>2</sub>O<sub>2</sub> and HOCl. In other words, the use of strong oxidants appears to create (transform) additional detectable compounds, of which the majority are subsequently destroyed by UV-AOP (89% for H<sub>2</sub>O<sub>2</sub> and 84% for HOCl per Figure 2). In the case of UV/NH<sub>2</sub>Cl, the total number of non-target features in the UVP sample was greater than that in the ROP sample, indicating worse performance of UV/NH<sub>2</sub>Cl in terms of the overall reduction of non-target feature counts (Figure 2a).

In terms of the summed peak area of non-target features from ROP to UVP, 62%, 74%, 13%, and 58% of the summed peak area was reduced by UV/HOCl, UV/H<sub>2</sub>O<sub>2</sub>, UV/NH<sub>2</sub>Cl, and UV/ambient, respectively (Figure 2b). Compared to the trend from non-target feature counts, where UV/HOCl and UV/H<sub>2</sub>O<sub>2</sub> performed similarly, the total peak area removal observations suggest that UV/H<sub>2</sub>O<sub>2</sub> reduced non-target feature counts to a greater extent.

Transformation products formed across the pilot system (non-target features in UVP that were not present in ROP) were also investigated (tan plus bright green in Figure 2a). There were 1810, 841, 2503, and 1941 non-target features formed across the pilot system with UV/HOCl, UV/H<sub>2</sub>O<sub>2</sub>, UV/NH<sub>2</sub>Cl, and UV/ambient, respectively. Totals of 44%, 26%, 80%, and 27% new products were formed when compared to the corresponding ROP samples, suggesting that UV/H<sub>2</sub>O<sub>2</sub> generated the least new products relative to the initial feed water.

In summary, samples were taken at three different points in the treatment train (prior to oxidant addition, after oxidant addition, and after UV-AOP), and UV/H<sub>2</sub>O<sub>2</sub> was the most favorable AOP with respect to the number of non-target features and their summed peak areas. UV/H<sub>2</sub>O<sub>2</sub> formed the least new transformation products upon oxidant addition based on number and percent formation (i.e., UVF compared to ROP) and had greater or similar performance to other oxidants with respect to non-target features removed and formed during UV-AOP (i.e., UVP compared to ROP or UVF). UV/H<sub>2</sub>O<sub>2</sub> also reduced the summed peak area to the greatest extent across the full treatment train.

**3.3. Elemental Composition of Assigned Organic Compounds.** Molecular formulae were assigned by MZmine 2 based on elemental compositions that result in the measured accurate mass. Molecular formulae were assignable to 84%, 87%, 84%, and 72% of the non-target features in MCX extracts of samples collected in 2018 under UV/HOCl, UV/H<sub>2</sub>O<sub>2</sub>, UV/NH<sub>2</sub>Cl, and UV/ambient conditions, respectively (Figure S3). Features for which no formulae were assigned are likely those which have elemental ratios outside of the assigned tolerances. The number of formulae across five classifications, including Cl-containing compounds, is depicted in Figure S4. Compounds containing only CHO or CHON were the most abundant of those classified, similar to other studies of organic matter occurring in drinking water and wastewater.<sup>25,58,59</sup> The transformations of organic compounds across ROP to UVP are depicted as van Krevelen diagrams in Figure 3. In terms of the

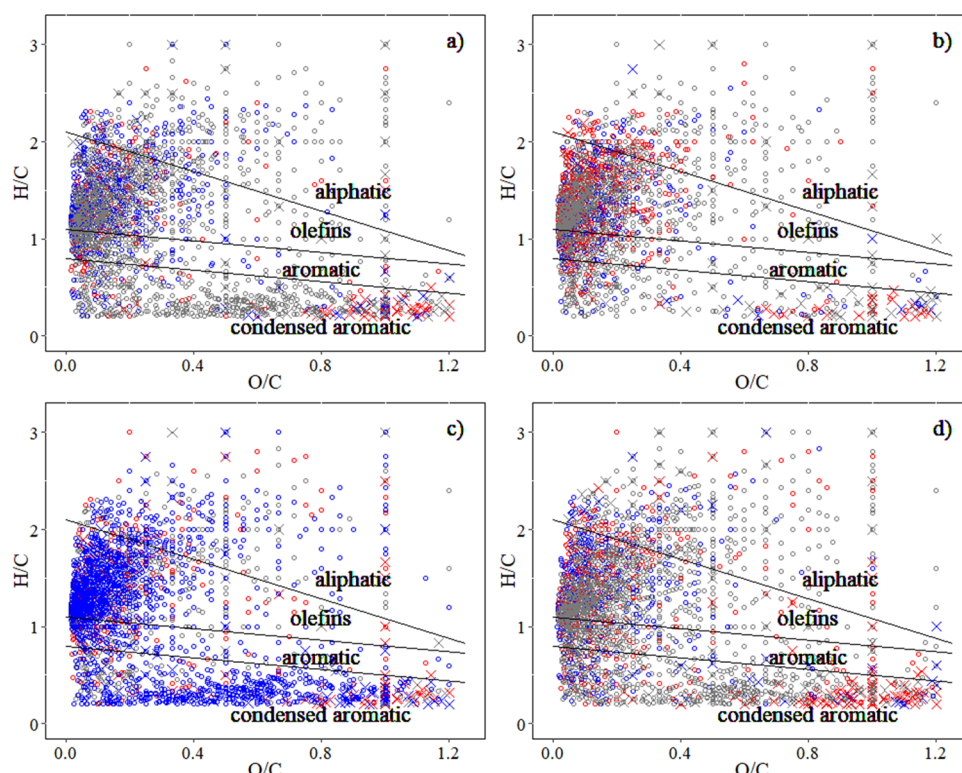


**Figure 3.** Van Krevelen diagrams of molecular formulae identified by LC-qTOF/MS during sampling conducted in 2018: a) UV/HOCl, b) UV/ $\text{H}_2\text{O}_2$ , c) UV/ $\text{NH}_2\text{Cl}$ , and d) UV/ambient. Red indicates persistent compounds (found in both ROP and UVP), blue indicates newly formed compounds (found in UVP but not in ROP), and gray indicates decomposed compounds (found in ROP but not in UVP). Circles indicate compounds without Cl and crosses indicate Cl-containing compounds. Cl-containing compounds include any combination of C, H, N, O, or S, and at least one Cl. The stoichiometric ranges used to establish the category boundaries are described in the Supporting Information.<sup>61,62</sup>

non-target features where formulae were assigned, UV/HOCl, UV/ $\text{H}_2\text{O}_2$ , and UV/ambient had similar removal (30–33%, the gray circle and cross) but UV/ $\text{NH}_2\text{Cl}$  increased the number of compounds with assigned formulae by 35%. This may be an artifact of the ~30% of the features that were not assigned a formula in the UV/ambient sample.

Of the degraded compounds across all oxidation conditions, olefins were decomposed to the greatest extent, likely due to the greater reactivity of unsaturated bonds, while aromatics tended to be decomposed the least (Figure S5a). Cl-containing compounds tended to be mostly aliphatic (over 44% over all treatments), followed by condensed aromatics (from 31–46%). There were 90, 77, 48, and 111 Cl-containing compounds decomposed by UV/HOCl, UV/ $\text{H}_2\text{O}_2$ , UV/ $\text{NH}_2\text{Cl}$ , and UV/ambient, accounting for 66%, 68%, 41%, and 43% Cl-containing compounds in the corresponding ROP samples. In the terms of summed peak area of Cl-containing compounds, UV/ $\text{H}_2\text{O}_2$  reduced the summed peak area to the greatest extent (74%), followed by UV/HOCl (46%) and UV/ambient (38%). The summed peak area increased when  $\text{NH}_2\text{Cl}$  was added as an oxidant due to increased Cl substitution (Figure S6). UV/ $\text{H}_2\text{O}_2$  produced the fewest number (52) of Cl-containing compounds in the UVP overall (however, noting that the ROP at that time featured overall smaller feature count), followed by UV/HOCl (86), UV/ $\text{NH}_2\text{Cl}$  (136), and UV/ambient (192). Together, these findings are highly relevant as Cl-containing compounds are thought to be responsible for a significant portion of the total toxic burden of disinfected waters, particularly when iodine concentrations are low.<sup>60</sup>

The molecular composition of transformation products (i.e., those features present in UVP, but not in ROP) was also evaluated. Similar to the conclusion regarding decomposed compounds, UV/ $\text{H}_2\text{O}_2$  generated the least fraction of transformation products (40% in UVP), nearly the same as the fraction generated when there was no supplemental oxidant (UV/ambient, 41%), compared to UV/ $\text{NH}_2\text{Cl}$  (~66%) and UV/HOCl (~70%). Of the transformation products, olefins were the largest group across all oxidant conditions (Figure S5b). UV/HOCl and UV/ $\text{H}_2\text{O}_2$  formed the least condensed aromatics, but aromatics were formed the least with UV/ $\text{NH}_2\text{Cl}$  and UV/ambient. Cl-containing transformation products tended to be condensed aromatics, followed by aliphatics. Similar to decomposed formulae, the least Cl-containing compounds were formed when  $\text{H}_2\text{O}_2$  was the oxidant (13% increase in Cl-containing compounds compared to UVP from ROP), followed by UV/ambient (18%), UV/HOCl (28%), and UV/ $\text{NH}_2\text{Cl}$  (59%). Overall, UV/ $\text{H}_2\text{O}_2$  formed the least Cl-containing transformation products and decomposed the greatest Cl-containing compounds present in the feed water to the UV-AOP.

**3.4. Bioassays.** Bioassays have been proposed for use in tandem with non-target analysis as an approach to assess potable reuse water quality once both methods become more standardized for water facility use.<sup>63</sup> A suite of bioassays (MTT, p53, SOS Chromotest, and ARE-Nrf2 assay; see Table S3 for details) were used to assess water quality before and after UV-AOP. HLB was used intentionally, rather than MCX used for NTA analysis, in an attempt to independently validate the conclusions from NTA. Finished drinking water from a

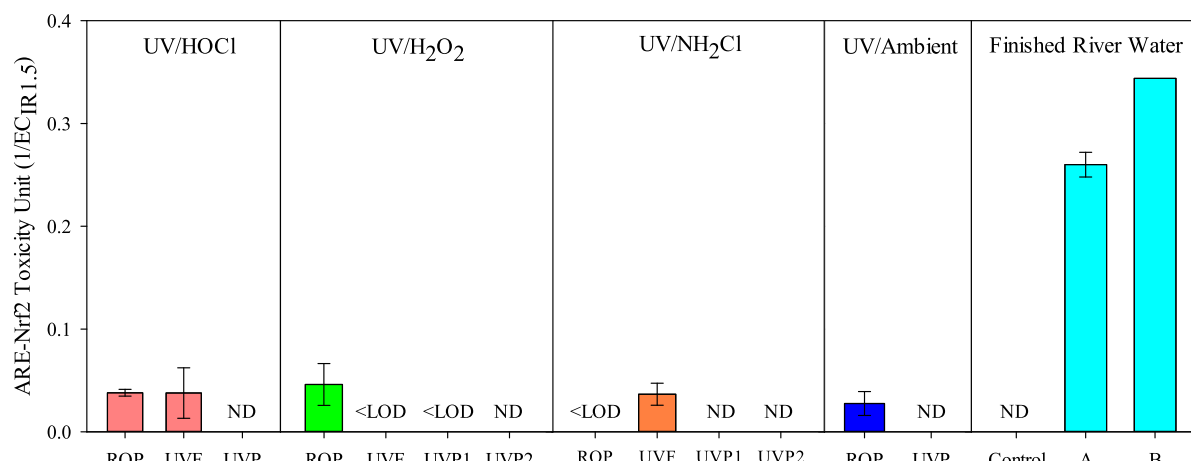


**Figure 4.** Oxidative stress response (ARE-Nrf2) of HLB extracts of samples collected in 2018. Finished river water from a conventional drinking water plant (A) is presented alongside finished river water from Australia (B).<sup>27</sup> UVP1 and UVP2 indicates 0 day hold UVP and 5 day hold UVP, respectively.

conventional drinking water treatment plant was also assayed and is presented for comparison. The MTT, p53, and SOS Chromotest assays did not elicit a toxicological response for any extract, indicating that the concentrations of toxic compounds was low in the HLB extracts. Further, concentration of the extracts tends to lead to the precipitation of organic matter, and thus, no further experimentation with these assays was conducted.

Extracts that elicited a response in the ARE-Nrf2 assay (the human cell-based assay targeting the activation of the oxidative stress response pathway) are presented in Figure 4 as unitless toxicity units (1/EC<sub>IR1.5</sub>). Based on the lack of response in the p53 and SOS bioassays, extracts that elicited an oxidative stress response via the ARE-Nrf2 assay did not have a significant impact on DNA. Three of the four ROP extracts elicited a response in the oxidative stress pathway (0.046, 0.038, and 0.028 TU). Based on comparison of ROP and UVF (i.e., after oxidant addition before UV treatment), for UV/H<sub>2</sub>O<sub>2</sub>, the application of H<sub>2</sub>O<sub>2</sub> attenuated the toxic response (0.046 TU to <LOD). For UV/HOCl, the response was comparable after HOCl addition (~0.038 TU). For UV/NH<sub>2</sub>Cl, the ROP that was initially non-reactive increased to detectable levels in the ARE-Nrf2 bioassay upon monochloramine addition (<LOD to 0.037 TU).

In all treatment scenarios, application of UV with any oxidant attenuated the oxidative stress response (Figure 4). This suggests that UV-AOP is effective at decomposing potentially toxic compounds that may be produced by oxidants during oxidant addition prior to UV and agrees well with the other findings in this study, suggesting that the oxidant addition prior to UV-AOP may create additional transformation products that are then decomposed during UV-AOP.

Filter effluent grab samples of river water treated with conventional treatment were disinfected in the laboratory by spiking with chlorine at a concentration mimicking the upper limit disinfection doses at full scale (5 mg Cl<sub>2</sub>/L, quenched after 24 h) and then were used for comparison. The ARE-Nrf2 assay again had a positive response (0.26 TU), which agreed with literature values for conventionally treated surface waters in Australia (0.344 TU<sup>27</sup>). Other assays did not elicit a response. Notably, the highest RO permeate responses (0.046 TU) in the present study are 86% less reactive than finished

treated “conventional” river waters from Australia. Many reporter gene assays are very sensitive and can detect an effect in clean water samples, including highly treated drinking water and bottled water.<sup>64,65</sup> Therefore, a response in an assay does not mean that the water quality is necessarily unacceptable, but the responses can be compared to literature values for qualitative comparison.

#### 4. CONCLUSIONS

Oxidants outside of traditional H<sub>2</sub>O<sub>2</sub> have recently been proposed as effective alternatives during UV-AOP. The performance of four different oxidant scenarios in terms of organic compound removal, organic compound production (transformation products), and bioassay-indicated toxicity were investigated in extracts produced from a UV-AOP pilot system at the Orange County Water District Advanced Water Purification Facility. Based on the results:

- Suspect compounds recovered by MCX cartridges from RO permeate that matched an in-house LC-qTOF/MS library were degraded more efficiently by UV/HOCl and UV/H<sub>2</sub>O<sub>2</sub> compared to UV/NH<sub>2</sub>Cl and UV/ambient chloramines.
- Based on the compounds present in MCX extracts and ionizable in ESI<sup>+</sup> mode, as measured by non-target analysis, UV/H<sub>2</sub>O<sub>2</sub> appears to be the most favorable AOP since it formed the least number and percentage of new transformation products in the UV feed water upon oxidant addition to the RO permeate (i.e., before UV exposure), had better or similar performance to other AOPs with respect to non-target features removed/formed across UV-AOP, and reduced the summed peak area to the greatest extent across the treatment train.
- Olefins were decomposed to the greatest extent, and aromatics were decomposed the most poorly. UV/H<sub>2</sub>O<sub>2</sub> formed the least Cl-containing transformation products and decomposed the greatest fraction of Cl-containing compounds.
- UV-AOP with any of the studied oxidants (HOCl, H<sub>2</sub>O<sub>2</sub>, and NH<sub>2</sub>Cl) produced water with a lower oxidative stress response (ARE-Nrf2) than conventionally treated drinking water (river water). The oxidative stress response in pre-AOP samples was mitigated to

below the assay response limit after UV-AOP. Samples that were positive in the ARE-Nrf2 assay did not elicit a response in four other assays measuring genetic stress or repair, indicating that the oxidative stress did not significantly impact the genetic material or induce cell death.

- Recognizing that feed water quality varies, reproduction of these results in additional experiments will advance the comparative assessment of oxidants used during AOP.
- It is important to consider these conclusions with recognition that the extraction of organic matter results in the potential for biased conclusions as no sorbent perfectly extracts all organic matter present. The non-target results presented here are biased toward organic bases (cation exchange extraction) because organic bases ionize well during electrospray positive. Further experimentation examining organic acids and neutrals should be conducted to improve our understanding of how these treatment methods affect the organic matter pool.

## ■ ASSOCIATED CONTENT

### SI Supporting Information

The Supporting Information is available free of charge at <https://pubs.acs.org/doi/10.1021/acsestwater.2c00485>.

Detailed analytical methods; (Figure S1) OCWD AWPF treatment process and sampling locations; (Figure S2) peak area of suspect compounds in MCX extracts of samples from 2019 ROP, UVF, and UVt treated by UV/HOCl and UV/H<sub>2</sub>O; (Figure S3) number of assigned and unassigned features under different oxidant additions from LC-qTOF/MS data produced from samples taken in 2018; (Figure S4) elemental composition of the organic compounds sampled in 2018 across the treatment system under varying oxidation conditions of samples extracted with MCX cartridges and analyzed by LC-qTOF/MS; (Figure S5) fractional representation of decomposed compounds and transformation products sampled in 2018 across the treatment system under varying oxidation conditions of samples extracted with MCX cartridges and analyzed by LC-qTOF/MS; (Figure S6) summed peak area of Cl-containing compounds across the treatment system under varying oxidation conditions of samples extracted with MCX cartridges and analyzed by LC-qTOF/MS; (Table S1) summary of samples and associated water quality; (Table S2) parameters of peak detection, EIC building, and peak picking for all data files; (Table S3) broad-spectrum bioassays used to assess water quality; (Table S4) suspect screening in all water samples; (Table S5) summed peak area of all suspect compounds in MCX extracts of samples from 2018 and 2019 sampling (PDF)

## ■ AUTHOR INFORMATION

### Corresponding Author

David Hanigan — Department of Civil and Environmental Engineering, University of Nevada, Reno, Nevada 89557-0258, United States; [orcid.org/0000-0002-6947-7611](https://orcid.org/0000-0002-6947-7611); Email: [DHanigan@unr.edu](mailto:DHanigan@unr.edu)

## Authors

Mingrui Song — Department of Civil and Environmental Engineering, University of Nevada, Reno, Nevada 89557-0258, United States; [orcid.org/0000-0003-1270-0904](https://orcid.org/0000-0003-1270-0904)

Elizabeth McKenna — Department of Civil and Environmental Engineering, University of Nevada, Reno, Nevada 89557-0258, United States; Present Address: Brown and Caldwell, 1527 Cole Blvd #300, Lakewood, Colorado 80401, United States

Imma Ferrer — Center for Environmental Mass Spectrometry, University of Colorado, Boulder, Colorado 80309, United States; [orcid.org/0000-0002-8730-7851](https://orcid.org/0000-0002-8730-7851)

E. Michael Thurman — Center for Environmental Mass Spectrometry, University of Colorado, Boulder, Colorado 80309, United States; [orcid.org/0000-0002-2191-1407](https://orcid.org/0000-0002-2191-1407)

Liz Taylor-Edmonds — Department of Civil Engineering, University of Toronto, Toronto, ON MSS 1A4, Canada

Ronald Hofmann — Department of Civil Engineering, University of Toronto, Toronto, ON MSS 1A4, Canada

Kenneth P. Ishida — Research & Development Department, Orange County Water District, Fountain Valley, California 92708, United States

Shannon L. Roback — School of Social Ecology, University of California, Irvine, California 92697, United States

Megan H. Plumlee — Research & Development Department, Orange County Water District, Fountain Valley, California 92708, United States

Complete contact information is available at:

<https://pubs.acs.org/10.1021/acsestwater.2c00485>

## Notes

The authors declare no competing financial interest.

## ■ ACKNOWLEDGMENTS

This research was supported by the National Science Foundation under Grant No. 1804255, the Water Research Foundation (Project No. 5005, managed by Djanette Khiari and Katie Spahr) and the United States Bureau of Reclamation Desalination and Water Purification Research Program.<sup>66</sup>

## ■ REFERENCES

- (1) Harris-Lovett, S. R.; Binz, C.; Sedlak, D. L.; Kiparsky, M.; Truffer, B. Beyond User Acceptance: A Legitimacy Framework for Potable Water Reuse in California. *Environ. Sci. Technol.* **2015**, *49*, 7552–7561.
- (2) Bixio, D.; Thoeye, C.; De Koning, J.; Joksimovic, D.; Savic, D.; Wintgens, T.; Melin, T. Wastewater reuse in Europe. *Desalination* **2006**, *187*, 89–101.
- (3) Gerrity, D.; Pecson, B.; Trussell, R. S.; Trussell, R. R. Potable reuse treatment trains throughout the world. *J. Water Supply: Res. Technol.-AQUA* **2013**, *62*, 321–338.
- (4) Board, C. S. W. R. C. *Terms and Definitions for Potable Reuse*. Available online from: [https://www.waterboards.ca.gov/drinking\\_water/certlic/drinkingwater/documents/recharge/ag\\_draft\\_recom\\_app\\_b.pdf](https://www.waterboards.ca.gov/drinking_water/certlic/drinkingwater/documents/recharge/ag_draft_recom_app_b.pdf); 2016.
- (5) Farhat, N. M.; Loubineaud, E.; Prest, E. I. E. C.; El-Chakhtoura, J.; Salles, C.; Bucs, S. S.; Trampé, J.; Van den Broek, W. B. P.; Van Agtmaal, J. M. C.; Van Loosdrecht, M. C. M.; et al. Application of monochloramine for wastewater reuse: Effect on biostability during transport and biofouling in RO membranes. *J. Membr. Sci.* **2018**, *551*, 243–253.
- (6) Kwon, M.; Royce, A.; Gong, Y.; Ishida, K. P.; Stefan, M. UV/Chlorine vs. UV/H<sub>2</sub>O<sub>2</sub> for water reuse at Orange County Water

District, CA: A pilot study. *Environ. Sci.: Water Res. Technol.* **2020**, 2416–2431.

(7) Zhang, Z.; Chuang, Y. H.; Szczuka, A.; Ishida, K. P.; Roback, S.; Plumlee, M. H.; Mitch, W. A. Pilot-scale evaluation of oxidant speciation, 1,4-dioxane degradation and disinfection byproduct formation during UV/hydrogen peroxide, UV/free chlorine and UV/chloramines advanced oxidation process treatment for potable reuse. *Water Res.* **2019**, 164, 114939.

(8) Zhang, Z.; Chuang, Y. H.; Huang, N.; Mitch, W. A. Predicting the Contribution of Chloramines to Contaminant Decay during Ultraviolet/Hydrogen Peroxide Advanced Oxidation Process Treatment for Potable Reuse. *Environ. Sci. Technol.* **2019**, 53, 4416–4425.

(9) Cao, Z.; Yu, X.; Zheng, Y.; Aghdam, E.; Sun, B.; Song, M.; Wang, A.; Han, J.; Zhang, J. Micropollutant abatement by the UV/chloramine process in potable water reuse: A review. *J. Hazard. Mater.* **2022**, 424, 127341.

(10) Wu, Z.; Chen, C.; Zhu, B.-Z.; Huang, C.-H.; An, T.; Meng, F.; Fang, J. Reactive Nitrogen Species Are Also Involved in the Transformation of Micropollutants by the UV/Monochloramine Process. *Environ. Sci. Technol.* **2019**, 53, 11142–11152.

(11) Wols, B. A.; Hofman-Caris, C. H.; Harmsen, D. J.; Beerendonk, E. F. Degradation of 40 selected pharmaceuticals by UV/H<sub>2</sub>O<sub>2</sub>. *Water Res.* **2013**, 47, 5876–5888.

(12) Li, W.; Xu, E.; Schlenk, D.; Liu, H. Cyto- and geno-toxicity of 1,4-dioxane and its transformation products during ultraviolet-driven advanced oxidation processes. *Environ. Sci.: Water Res. Technol.* **2018**, 4, 1213–1218.

(13) Mariani, M. L.; Romero, R. L.; Zalazar, C. S. Modeling of degradation kinetic and toxicity evaluation of herbicides mixtures in water using the UV/H<sub>2</sub>O<sub>2</sub> process. *Photochem. Photobiol. Sci.* **2015**, 14, 608–617.

(14) Sharma, A.; Ahmad, J.; Flora, S. J. S. Application of advanced oxidation processes and toxicity assessment of transformation products. *Environ. Res.* **2018**, 167, 223–233.

(15) Roback, S. L.; Ishida, K. P.; Plumlee, M. H. Influence of reverse osmosis membrane age on rejection of NDMA precursors and formation of NDMA in finished water after full advanced treatment for potable reuse. *Chemosphere* **2019**, 233, 120–131.

(16) Roback, S. L.; Ferrer, I.; Thurman, E. M.; Ishida, K. P.; Plumlee, M. H.; Poustie, A.; Westerhoff, P.; Hanigan, D. Non-target mass spectrometry analysis of NDMA precursors in advanced treatment for potable reuse. *Environ. Sci.: Water Res. Technol.* **2018**, 4, 1944–1955.

(17) Huang, Y.; Kong, M.; Coffin, S.; Cochran, K. H.; Westerman, D. C.; Schlenk, D.; Richardson, S. D.; Lei, L.; Dionysiou, D. D. Degradation of contaminants of emerging concern by UV/H<sub>2</sub>O<sub>2</sub> for water reuse: Kinetics, mechanisms, and cytotoxicity analysis. *Water Res.* **2020**, 174, 115587.

(18) Chuang, Y. H.; Wu, K. L.; Lin, W. C.; Shi, H. J. Photolysis of Chlorine Dioxide under UVA Irradiation: Radical Formation, Application in Treating Micropollutants, Formation of Disinfection Byproducts, and Toxicity under Scenarios Relevant to Potable Reuse and Drinking Water. *Environ. Sci. Technol.* **2022**, 2593–2604.

(19) Chuang, Y.-H.; Shi, H.-J. UV/chlorinated cyanurates as an emerging advanced oxidation process for drinking water and potable reuse treatments. *Water Res.* **2022**, 211, 118075.

(20) Escher, B. I.; van Daele, C.; Dutt, M.; Tang, J. Y.; Altenburger, R. Most oxidative stress response in water samples comes from unknown chemicals: the need for effect-based water quality trigger values. *Environ. Sci. Technol.* **2013**, 47, 7002–7011.

(21) Hanigan, D.; Truong, L.; Simonich, M.; Tanguay, R.; Westerhoff, P. Zebrafish embryo toxicity of 15 chlorinated, brominated, and iodinated disinfection by-products. *J. Environ. Sci.* **2017**, 58, 302–310.

(22) Schymanski, E. L.; Singer, H. P.; Slobodnik, J.; Ipolyi, I. M.; Oswald, P.; Krauss, M.; Schulze, T.; Haglund, P.; Letzel, T.; Grosse, S.; et al. Non-target screening with high-resolution mass spectrometry: critical review using a collaborative trial on water analysis. *Anal. Bioanal. Chem.* **2015**, 407, 6237–6255.

(23) Albergamo, V.; Escher, B. I.; Schymanski, E. L.; Helmus, R.; Dingemans, M. M. L.; Cornelissen, E. R.; Kraak, M. H. S.; Hollender, J.; de Voogt, P. Evaluation of reverse osmosis drinking water treatment of riverbank filtrate using bioanalytical tools and non-target screening. *Environ. Sci.: Water Res. Technol.* **2020**, 6, 103–116.

(24) Soliman, M. A.; Pedersen, J. A.; Park, H.; Castaneda-Jimenez, A.; Stenstrom, M. K.; Suffet, I. H. Human pharmaceuticals, antioxidants, and plasticizers in wastewater treatment plant and water reclamation plant effluents. *Water Environ. Res.* **2007**, 79, 156–167.

(25) Ishida, K. P.; Luna, R. F.; Richardot, W. H.; Lopez-Galvez, N.; Plumlee, M. H.; Dodder, N. G.; Hoh, E. Nontargeted Analysis of Trace Organic Constituents in Reverse Osmosis and UV-AOP Product Waters of a Potable Reuse Facility. *ACS EST Water* **2022**, 96–105.

(26) Tang, J. Y. M.; Busetti, F.; Charrois, J. W. A.; Escher, B. I. Which chemicals drive biological effects in wastewater and recycled water? *Water Res.* **2014**, 60, 289–299.

(27) Escher, B. I.; Allinson, M.; Altenburger, R.; Bain, P. A.; Balaguer, P.; Busch, W.; Crago, J.; Denslow, N. D.; Dopp, E.; Hilscherova, K.; et al. Benchmarking organic micropollutants in wastewater, recycled water and drinking water with in vitro bioassays. *Environ. Sci. Technol.* **2014**, 48, 1940–1956.

(28) Escher, B.; Leusch, F. *Bioanalytical tools in water quality assessment*; IWA publishing: 2011.

(29) Neale, P. A.; Antony, A.; Bartkow, M. E.; Farré, M. J.; Heitz, A.; Kristiana, I.; Tang, J. Y. M.; Escher, B. I. Bioanalytical assessment of the formation of disinfection byproducts in a drinking water treatment plant. *Environ. Sci. Technol.* **2012**, 46, 10317–10325.

(30) McKenna, E.; Thompson, K. A.; Taylor-Edmonds, L.; McCurry, D. L.; Hanigan, D. Summation of disinfection by-product CHO cell relative toxicity indices: sampling bias, uncertainty, and a path forward. *Environ. Sci.: Processes Impacts* **2020**, 22, 708–718.

(31) Lau, S. S.; Wei, X.; Bokenkamp, K.; Wagner, E. D.; Plewa, M. J.; Mitch, W. A. Assessing Additivity of Cytotoxicity Associated with Disinfection Byproducts in Potable Reuse and Conventional Drinking Waters. *Environ. Sci. Technol.* **2020**, 54, 5729–5736.

(32) Liu, C.; Shin, Y.-H.; Wei, X.; Ersan, M. S.; Wagner, E.; Plewa, M. J.; Amy, G.; Karanfil, T. Preferential Halogenation of Algal Organic Matter by Iodine over Chlorine and Bromine: Formation of Disinfection Byproducts and Correlation with Toxicity of Disinfected Waters. *Environ. Sci. Technol.* **2022**, 1244–1256.

(33) Huynh, N.; Caupos, E.; Soares Peirera, C.; Le Roux, J.; Bressy, A.; Moilleron, R. Evaluation of Sample Preparation Methods for Non-Target Screening of Organic Micropollutants in Urban Waters Using High-Resolution Mass Spectrometry. *Molecules* **2021**, 7064.

(34) Baker, D. R.; Kasprzyk-Hordern, B. Critical evaluation of methodology commonly used in sample collection, storage and preparation for the analysis of pharmaceuticals and illicit drugs in surface water and wastewater by solid phase extraction and liquid chromatography–mass spectrometry. *J. Chromatogr. A* **2011**, 1218, 8036–8059.

(35) Hanigan, D.; Liao, X.; Zhang, J.; Herckes, P.; Westerhoff, P. Sorption and desorption of organic matter on solid-phase extraction media to isolate and identify N-nitrosodimethylamine precursors. *J. Sep. Sci.* **2016**, 39, 2796–2805.

(36) González-Mariño, I.; Quintana, J. B.; Rodríguez, I.; Rodil, R.; González-Peñas, J.; Cela, R. Comparison of molecularly imprinted, mixed-mode and hydrophilic balance sorbents performance in the solid-phase extraction of amphetamine drugs from wastewater samples for liquid chromatography-tandem mass spectrometry determination. *J. Chromatogr. A* **2009**, 1216, 8435–8441.

(37) Jeong, Y.; Schäffer, A.; Smith, K. Equilibrium partitioning of organic compounds to OASIS HLB((R)) as a function of compound concentration, pH, temperature and salinity. *Chemosphere* **2017**, 174, 297–305.

(38) Mackey, E. D.; Hofmann, R.; Festger, A.; Vanyo, C. *UV-Chlorine AOP in Potable Reuse: A Guidance Manual to Assessment and Implementation (Report No. S050)*; The Water Research Foundation,

2022. <https://www.waterrf.org/research/projects/uvchlorine-aop-potable-reuse-assessment-applicability-operational-issues-and>.

(39) Sun, P.; Meng, T.; Wang, Z.; Zhang, R.; Yao, H.; Yang, Y.; Zhao, L. Degradation of Organic Micropollutants in UV/NH<sub>2</sub>Cl Advanced Oxidation Process. *Environ. Sci. Technol.* **2019**, *53*, 9024–9033.

(40) Jiang, B.; Tian, Y.; Zhang, Z.; Yin, Z.; Feng, L.; Liu, Y.; Zhang, L. Degradation behaviors of Isopropylphenazone and Aminopyrine and their genetic toxicity variations during UV/chloramine treatment. *Water Res.* **2020**, *170*, 115339.

(41) Zheng, D.; Andrews, R. C.; Andrews, S. A.; Taylor-Edmonds, L. Effects of coagulation on the removal of natural organic matter, genotoxicity, and precursors to halogenated furanones. *Water Res.* **2015**, *70*, 118–129.

(42) Myers, O. D.; Sumner, S. J.; Li, S.; Barnes, S.; Du, X. One Step Forward for Reducing False Positive and False Negative Compound Identifications from Mass Spectrometry Metabolomics Data: New Algorithms for Constructing Extracted Ion Chromatograms and Detecting Chromatographic Peaks. *Anal. Chem.* **2017**, *89*, 8696–8703.

(43) Verkh, Y.; Rozman, M.; Petrovic, M. Extraction and cleansing of data for a non-targeted analysis of high-resolution mass spectrometry data of wastewater. *MethodsX* **2018**, *5*, 395–402.

(44) Pluskal, T.; Uehara, T.; Yanagida, M. Highly accurate chemical formula prediction tool utilizing high-resolution mass spectra, MS/MS fragmentation, heuristic rules, and isotope pattern matching. *Anal. Chem.* **2012**, *84*, 4396–4403.

(45) R Core Team. *R: A Language and Environment for Statistical Computing*; R Foundation for Statistical Computing: Vienna, Austria; 2019.

(46) Sun, J.; Peng, H.; Alharbi, H. A.; Jones, P. D.; Giesy, J. P.; Wiseman, S. B. Identification of Chemicals that Cause Oxidative Stress in Oil Sands Process-Affected Water. *Environ. Sci. Technol.* **2017**, *51*, 8773–8781.

(47) Pluquet, O.; Hainaut, P. Genotoxic and non-genotoxic pathways of p53 induction. *Cancer Lett.* **2001**, *174*, 1–15.

(48) Escher, B. I.; Dutt, M.; Maylin, E.; Tang, J. Y.; Toze, S.; Wolf, C. R.; Lang, M. Water quality assessment using the AREc32 reporter gene assay indicative of the oxidative stress response pathway. *J. Environ. Monit.* **2012**, *14*, 2877–2885.

(49) Hanigan, D.; Ferrer, I.; Thurman, E. M.; Herkes, P.; Westerhoff, P. LC/QTOF-MS fragmentation of N-nitrosodimethylamine precursors in drinking water supplies is predictable and aids their identification. *J. Hazard. Mater.* **2017**, *323*, 18–25.

(50) Ferrer, I.; Thurman, E. M. Analysis of 100 pharmaceuticals and their degradates in water samples by liquid chromatography/quadrupole time-of-flight mass spectrometry. *J. Chromatogr. A* **2012**, *1259*, 148–157.

(51) Ferrer, I.; Thurman, E. M. Multi-residue method for the analysis of 101 pesticides and their degradates in food and water samples by liquid chromatography/time-of-flight mass spectrometry. *J. Chromatogr. A* **2007**, *1175*, 24–37.

(52) Gao, Y.-Q.; Gao, N.-Y.; Chen, J.-X.; Zhang, J.; Yin, D.-Q. Oxidation of  $\beta$ -blocker atenolol by a combination of UV light and chlorine: Kinetics, degradation pathways and toxicity assessment. *Sep. Purif. Technol.* **2020**, *231*, 115927.

(53) Yang, T.; Mai, J.; Wu, S.; Liu, C.; Tang, L.; Mo, Z.; Zhang, M.; Guo, L.; Liu, M.; Ma, J. UV/chlorine process for degradation of benzothiazole and benzotriazole in water: Efficiency, mechanism and toxicity evaluation. *Sci. Total Environ.* **2021**, *760*, 144304.

(54) Nam, S. W.; Yoon, Y.; Choi, D. J.; Zoh, K. D. Degradation characteristics of metoprolol during UV/chlorination reaction and a factorial design optimization. *J. Hazard. Mater.* **2015**, *285*, 453–463.

(55) Tian, F. X.; Ye, W. K.; Xu, B.; Hu, X. J.; Ma, S. X.; Lai, F.; Gao, Y. Q.; Xing, H. B.; Xia, W. H.; Wang, B. Comparison of UV-induced AOPs (UV/Cl<sub>2</sub>, UV/NH<sub>2</sub>Cl, UV/ClO<sub>2</sub> and UV/H<sub>2</sub>O<sub>2</sub>) in the degradation of iopamidol: Kinetics, energy requirements and DBPs-related toxicity in sequential disinfection processes. *Chem. Eng. J.* **2020**, *398*, 125570.

(56) Chen, C.-Y. The Oxidation of Di-(2-Ethylhexyl) Phthalate (DEHP) in Aqueous Solution by UV/H<sub>2</sub>O<sub>2</sub> Photolysis. *Water, Air, Soil Pollut.* **2010**, *209*, 411–417.

(57) Thurman, E. M.; Ferrer, I.; Barceló, D. Choosing between Atmospheric Pressure Chemical Ionization and Electrospray Ionization Interfaces for the HPLC/MS Analysis of Pesticides. *Anal. Chem.* **2001**, *73*, 5441–5449.

(58) Maizel, A. C.; Remucal, C. K. The effect of advanced secondary municipal wastewater treatment on the molecular composition of dissolved organic matter. *Water Res.* **2017**, *122*, 42–52.

(59) Qian, Y.; Chen, Y.; Hanigan, D.; Shi, Y.; Sun, S.; Hu, Y.; An, D. pH adjustment improves the removal of disinfection byproduct precursors from sedimentation sludge water. *Resour., Conserv. Recycl.* **2022**, *179*, 106135.

(60) Allen, J. M.; Plewa, M. J.; Wagner, E. D.; Wei, X.; Bokenkamp, K.; Hur, K.; Jia, A.; Liberatore, H. K.; Lee, C. T.; Shirkhani, R.; Krasner, S. W.; Richardson, S. D. Drivers of Disinfection Byproduct Cytotoxicity in U.S. Drinking Water: Should Other DBPs Be Considered for Regulation? *Environ. Sci. Technol.* **2022**, *392*–402.

(61) Kellerman, A. M.; Dittmar, T.; Kothawala, D. N.; Tranvik, L. J. Chemodiversity of dissolved organic matter in lakes driven by climate and hydrology. *Nat. Commun.* **2014**, *5*, 3804.

(62) Varanasi, L.; Coscarelli, E.; Khaksari, M.; Mazzoleni, L. R.; Minakata, D. Transformations of dissolved organic matter induced by UV photolysis, Hydroxyl radicals, chlorine radicals, and sulfate radicals in aqueous-phase UV-Based advanced oxidation processes. *Water Res.* **2018**, *135*, 22–30.

(63) Snyder, S. A. Emerging chemical contaminants: Looking for greater harmony. *J. - Am. Water Works Assoc.* **2014**, *106*, 38–52.

(64) Neale, P. A.; Escher, B. I. In vitro bioassays to assess drinking water quality. *Curr. Opin. Environ. Sci. Health* **2019**, *7*, 1–7.

(65) Hebert, A.; Feliers, C.; Lecarpentier, C.; Neale, P. A.; Schlichting, R.; Thibert, S.; Escher, B. I. Bioanalytical assessment of adaptive stress responses in drinking water: A predictive tool to differentiate between micropollutants and disinfection by-products. *Water Res.* **2018**, *132*, 340–349.

(66) Roback, S.; Plumlee, M. H.; Hanigan, D.; Song, M.; Mckenna, L. *Understanding the Formation of a Critical Disinfection Byproduct: NDMA and NDMA Precursors in Advanced Potable Reuse Treatment Plants (Report No. 222)*; Orange County Water District, CA. Online Link: [https://www.usbr.gov/research/dwpr/DWPR\\_Reports.html](https://www.usbr.gov/research/dwpr/DWPR_Reports.html), 2022.